

# CMB anisotropies and linear matter power spectrum in models with non-thermal neutrinos and primordial magnetic fields

Kerstin E. Kunze\*

*Departamento de Física Fundamental, Universidad de Salamanca,  
Plaza de la Merced s/n, 37008 Salamanca, Spain*

(Dated: June 2, 2021)

Angular power spectra of temperature anisotropies and polarization of the cosmic microwave background (CMB) as well as the linear matter power spectra are calculated for models with three light neutrinos with non-thermal phase-space distributions in the presence of a primordial stochastic magnetic field. The non-thermal phase-space distribution function is assumed to be the sum of a Fermi-Dirac and a gaussian distribution. It is found that the known effective description of the non-thermal model in terms of a twin thermal model with extra relativistic degrees of freedom can also be extended to models including a stochastic magnetic field. Numerical solutions are obtained for a range of magnetic field parameters.

## I. INTRODUCTION

The standard model of cosmology predicts the presence of a cosmic neutrino background. Direct detection is very difficult. Neutrinos in the standard model are light and have a thermal distribution. Observations of solar as well as atmospheric neutrino oscillations put bounds on the mass differences. Depending on which mass difference is assigned between the two lowest neutrino masses the mass hierarchy is either normal or inverted. Effectively, this results in either two lighter neutrinos and one more massive or vice versa. Distinguishing between the mass hierarchies is very challenging as the mass differences are extremely small. However, in principle it might be possible using cosmological observations as neutrinos with different masses have slightly different decoupling temperatures. Light neutrinos act as non cold dark matter. The main effect is the suppression of the linear matter power spectrum on small scales due to free-streaming (for reviews, e.g., [1–5]).

Primordial magnetic fields have the opposite effect on the matter power spectrum. The Lorentz term in the baryon velocity equation drives the evolution of the baryon and consequently the dark

---

\* kkunze@usal.es

matter perturbation causing the domination over the adiabatic, primordial curvature mode on small scales [6–9]. Primordial magnetic fields generated in the very early universe, e.g. during inflation or at a phase transition, are generally constrained to be less or of order nG, in terms of their present day comoving field strength (e.g., [10]). Taking into account the evolution of cosmic magnetic fields due to their interaction with the cosmic plasma, leading to damping by decaying magnetohydrodynamic turbulence shortly after photon decoupling or ambipolar diffusion important in partially ionized matter, before the epoch of reionization, much stronger constraints have been derived. This is due to the additional heating of matter by the dissipating magnetic field [7, 11, 12]

Within the standard model of cosmology neutrinos are in thermal equilibrium with the rest of the cosmic plasma upto their decoupling when the universe cooled down to about 1 MeV resulting in the postulated cosmic neutrino background ( $C\nu B$ ). The Fermi-Dirac distribution could include a non zero chemical potential which, however, can be constrained by Big Bang Nucleosynthesis (BBN). In addition neutrinos could be created at a much later stage by particle decay. In this case their distribution could be non-thermal. Modelling this non-thermal contribution as a gaussian it has been shown in [13] that the non-thermal model can be described in terms of a "twin" model with thermal neutrinos and extra (relativistic) degrees of freedom. Thereby allowing for a degeneracy between this type of non-thermal  $C\nu B$  and a thermal counterpart in a cosmic background with extra relativistic degrees of freedom. It is this model of non-thermal neutrinos which will be used here in backgrounds with a primordial stochastic magnetic field.

There are several open source programs available to calculate the CMB anisotropies and the matter power spectrum, such as COSMICS [14], CMBFAST [15], CAMB [16], CMBEASY [17] and CLASS [18–22]. The numerical solutions are obtained here by modifying the CLASS code.

In section II details of the non-thermal neutrino phase-space distribution function and the contribution of the primordial stochastic magnetic field are provided. Results are given in section III. Section IV contains the conclusions.

## II. MODELLING NON-THERMAL NEUTRINOS AND PRIMORDIAL MAGNETIC FIELDS

In this section details of the model under consideration will be given.

### A. Non-thermal neutrinos

Within the standard model of cosmology BBN constrains the thermal evolution of the universe and predicts the creation of the thermal CνB at around 1 MeV. Following [13] it is assumed that a non-thermal contribution to the CνB is created by the decay of a light neutral scalar particle  $\Phi$  with mass  $M$  producing active neutrinos of the same type as in the standard model after the weak interaction freeze-out and before photon decoupling. The latter ensures that the CMB anisotropies and the linear matter power spectrum are directly affected. The simplest model considers an out-of-equilibrium, instantaneous decay scenario  $\Phi \rightarrow \bar{\nu}\nu$  taking place when the CνB is at a temperature  $T_D$ . Upto that moment the neutrinos of the CνB are determined by a Fermi-Dirac distribution function with zero chemical potential in the simplest model of standard cosmology. With the sudden decay of the  $\Phi$  particle and production of neutrinos the neutrino distribution function receives a non-thermal contribution. In [13] this is modelled by a gaussian distribution function. In particular, it is assumed that for each mass eigenstate the total neutrino distribution function  $f(y)$  is given by

$$y^2 f(y) = y^2 \frac{1}{e^y + 1} dy + y^2 \frac{A}{\sqrt{2\pi\sigma^2}} \exp \left[ - \left( \frac{y - y_*}{2\sigma^2} \right)^2 \right], \quad (2.1)$$

where the  $y = ka$  is the comoving neutrino momentum. The first term is the Fermi-Dirac distribution with zero chemical potential for the thermal part and the second one the non-thermal distribution function which is strongly peaked at  $y_*$  given by  $y_* = \frac{M}{2T_D}$  and  $\sigma \ll y_*$ .

In general the moments of a phase-space distribution can be used to calculate physical variables. Following [13] the moments for a neutrino mass state  $\alpha$  are defined by

$$Q_\alpha^{(n)} = \frac{1}{\pi^2} \left( \frac{4}{11} \right)^{\frac{3+n}{3}} T_\gamma^{3+n} \int y^{2+n} f_\alpha(y) dy \quad (2.2)$$

where  $T_\gamma$  is the photon temperature. For  $\alpha$  neutrino mass states the effective number of neutrinos,  $N_{eff}$  is given by [13]

$$N_{eff} = \frac{120}{7\pi^2} \left( \frac{11}{4} \right)^{\frac{4}{3}} T_\gamma^{-4} \sum_\alpha Q_\alpha^{(1)}, \quad (2.3)$$

Assuming that all neutrino mass states have the same phase-space distribution function the neutrino density parameter  $\omega_\nu = \Omega_\nu h^2$ , can be expressed as, suppressing the index  $\alpha$ ,

$$\omega_\nu = \frac{m_0}{94.1[93.2]\text{eV}} \frac{2\pi^2}{3\zeta(3)} \frac{11}{4} T_\gamma^{-3} Q^{(0)} \quad (2.4)$$

where the total mass  $m_0$  is written in terms of the standard value for thermal neutrinos with a Fermi-Dirac distribution with zero chemical potential for, respectively,  $N_{eff} = 3$  and the number in brackets for  $N_{eff} = 3.04$  resulting from more precise numerical solutions including heating during the electron-positron annihilation phase [1, 13]. As pointed out in [13] cosmological data provide the strongest constraints on  $N_{eff}$  and  $\omega_\nu$ . Therefore only the first two moments will be taken into account. A positive amplitude  $A$  in the total neutrino distribution function increases  $N_{eff}$  as well as  $\omega_\nu$ . However, adjusting different parameters in the model allows to find correspondences with different kind of cosmological models. Namely, the observational implications of the three non-thermal neutrino model under consideration here can effectively be obtained from a three thermal neutrino model with extra relativistic degrees of freedom [2, 13, 23].

In particular, adjusting the present day value of the neutrino temperature, the neutrino masses as well as the cold dark matter density parameter,  $\omega_c$ , allows to tune  $N_{eff}$ ,  $\omega_\nu$  as well as the redshift of radiation-matter equality,  $z_{eq}$ . The first two changes yield the three thermal neutrino model corresponding to the non-thermal one. A larger  $N_{eff}$  leads to a potentially significant change in  $z_{eq}$  and hence the amplitude of the first peaks in the angular power spectrum of the CMB anisotropies. This can be prevented by adjusting  $\omega_c$  accordingly [2, 24–26].

## B. Primordial magnetic fields

Primordial magnetic fields present from before decoupling have a direct influence on the CMB anisotropies as well as the matter power spectrum determining large scale structure (LSS) (e.g. [6, 27–29]). This is due to the magnetic energy density perturbation with amplitude in Fourier space,  $\Delta_B(\vec{k})$ , as well as the anisotropic stress perturbation,  $\pi_B(\vec{k})$ . Moreover, the Lorentz term with amplitude in Fourier space,

$$L(\vec{k}) = \Delta_B(\vec{k}) - \frac{2}{3}\pi_B(\vec{k}), \quad (2.5)$$

in the evolution equation of the baryon velocity causes the rise in the matter power spectrum on small scales. Assuming a nonhelical, random Gaussian magnetic field its two-point function in  $k$ -space is chosen to be (e.g., [28])

$$\langle B_i^*(\vec{k})B_j(\vec{q}) \rangle = (2\pi)^3 \delta(\vec{k} - \vec{q}) P_B(k) \left( \delta_{ij} - \frac{k_i k_j}{k^2} \right), \quad (2.6)$$

where the power spectrum,  $P_B(k)$ , is assumed to be a power law,  $P_B(k) = A_B k^{n_B}$ , with amplitude,  $A_B$ , and spectral index,  $n_B$ . The ensemble average energy density of the magnetic field is defined using a Gaussian window function so that

$$\langle \rho_{B,0} \rangle = \int \frac{d^3 k}{(2\pi)^3} P_{B,0}(k) e^{-2\left(\frac{k}{k_c}\right)^2}, \quad (2.7)$$

where  $k_c$  is a certain Gaussian smoothing scale and a "0" refers to the present epoch. The magnetic field is treated as frozen-in with the cosmic fluid. This implies that its energy density scales with the scale factor  $a$  as  $a^{-4}$ . Effectively, this is implemented by defining the Fourier transformations of the magnetic energy density and anisotropic stress in terms of the photon energy density, yielding time independent Fourier amplitudes,  $\Delta_B(\vec{k})$  and  $\pi_B(\vec{k})$ , respectively. Moreover, the magnetic field power spectrum can be conveniently expressed in terms of  $\rho_{B,0}$  resulting in

$$P_{B,0}(k) = \frac{4\pi^2}{k_c^3} \frac{2^{(n_B+3)/2}}{\Gamma\left(\frac{n_B+3}{2}\right)} \left(\frac{k}{k_c}\right)^{n_B} \langle \rho_{B,0} \rangle. \quad (2.8)$$

The case  $n_B = 3$  corresponds to the scale-invariant case for which the contribution to the energy density per logarithmic wavenumber is independent of wave number. Primordial magnetic fields interact with the cosmic plasma. This leads to a damping of the magnetic field. Before decoupling this is due to photon viscosity, a process similar to the damping of density perturbations by photon diffusion, i.e. Silk damping. For a frozen-in magnetic field this is commonly modelled by a maximal wave number  $k_m$  determined by the Alfvén velocity and photon diffusion scale at decoupling [30, 31]

$$k_m = \frac{299.66}{\cos \theta} \left(\frac{B_0}{\text{nG}}\right)^{-1} \text{Mpc}^{-1} \quad (2.9)$$

for the best-fit values of  $\Lambda$ CDM derived from the Planck13+WP data. For simplicity the direction cosine of the wave vector and the magnetic field vector  $\cos \theta$  is set to 1 [12]. The Gaussian smoothing scale will be set to the maximal damping wave number,  $k_c \equiv k_m$ .

Linear cosmological perturbations induced by a primordial magnetic field can be separated into two contributions, namely one that is proportional to  $\Delta_B(\vec{k})$  and one that is proportional to  $\pi_B(\vec{k})$ . The total CMB angular power spectra as well as the linear matter power spectrum are determined by the two-point functions of the corresponding random variables of  $\Delta_B(\vec{k})$  and  $\pi_B(\vec{k})$  and their auto- and cross correlation functions, respectively. For massless, thermal neutrinos numerical solutions with the magnetic field correlation functions calculated with a Gaussian window function as described above have been obtained with a modified version of CMBEASY for nonhelical [28] as well as helical fields for scalar, vector and tensor modes [32].

In [28] the power spectra determining the two-point correlation functions in  $k$ -space of the magnetic energy density and the anisotropic stress in the scalar sector have been calculated. These are expressed in terms of the dimensionless power spectrum  $\mathcal{P}_{FG}(k)$  which determines the two-point function

$$\langle F_{\vec{k}}^* G_{\vec{k}'} \rangle = \frac{2\pi^2}{k^3} \mathcal{P}_{(FG)}(k) \delta_{\vec{k}, \vec{k}'} \quad (2.10)$$

of two random variables  $F$  and  $G$ . The autocorrelation function of the magnetic energy density is determined by the dimensionless power spectrum

$$\begin{aligned} \mathcal{P}_{\langle \Delta_B \Delta_B \rangle}(k, k_m) &= \frac{1}{[\Gamma(\frac{n_B+3}{2})]^2} \left[ \frac{\rho_{B0}}{\rho_{\gamma 0}} \right]^2 \left( \frac{k}{k_m} \right)^{2(n_B+3)} e^{-\left(\frac{k}{k_m}\right)^2} \int_0^\infty dz z^{n_B+2} e^{-2\left(\frac{k}{k_m}\right)^2 z^2} \\ &\quad \int_{-1}^1 dx e^{2\left(\frac{k}{k_m}\right)^2 zx} (1 - 2zx + z^2)^{\frac{n_B-2}{2}} (1 + x^2 + 2z^2 - 4zx), \end{aligned} \quad (2.11)$$

where  $x \equiv \vec{k} \cdot \vec{q}/kq$  and  $z \equiv \frac{q}{k}$ . Moreover, using the average energy density of the magnetic field (cf. equation (2.7)) leads to  $\frac{\rho_{B,0}}{\rho_{\gamma,0}} = 9.545 \times 10^{-8} \left(\frac{B_0}{nG}\right)^2$ .

The numerical solution of  $\mathcal{P}_{\langle \Delta_B \Delta_B \rangle}(k, k_m)$  (cf. equation (2.11)) can be approximated by the numerical fitting formula

$$\begin{aligned} \mathcal{P}_{\langle \Delta_B \Delta_B \rangle}(k, k_m) &= \frac{1}{[\Gamma(\frac{n_B+3}{2})]^2} \left[ \frac{\rho_{B0}}{\rho_{\gamma 0}} \right]^2 \left( \frac{k}{k_m} \right)^{2(n_B+3)} e^{-\left(\frac{k}{k_m}\right)^2} \\ &\quad \times 4.09512 (n_B + 3.1)^{-1.16608}. \end{aligned} \quad (2.12)$$

The autocorrelation function of the magnetic anisotropic stress is determined by the dimensionless spectrum [28]

$$\begin{aligned} \mathcal{P}_{\langle \pi_B \pi_B \rangle}(k, k_m) &= \frac{9}{[\Gamma(\frac{n_B+3}{2})]^2} \left[ \frac{\rho_{B0}}{\rho_{\gamma 0}} \right]^2 \left( \frac{k}{k_m} \right)^{2(n_B+3)} e^{-\left(\frac{k}{k_m}\right)^2} \int_0^\infty dz z^{n_B+2} e^{-2\left(\frac{k}{k_m}\right)^2 z^2} \\ &\quad \int_{-1}^1 dx e^{2\left(\frac{k}{k_m}\right)^2 zx} (1 - 2zx + z^2)^{\frac{n_B-2}{2}} (1 + 5z^2 + 2zx + (1 - 12z^2)x^2 - 6zx^3 + 9z^2x^4). \end{aligned} \quad (2.13)$$

The numerical solution for  $\mathcal{P}_{\langle \pi_B \pi_B \rangle}(k, k_m)$  can be approximated by the numerical fitting formula,

$$\begin{aligned} \mathcal{P}_{\langle \pi_B \pi_B \rangle}(k, k_m) &= \frac{9}{[\Gamma(\frac{n_B+3}{2})]^2} \left[ \frac{\rho_{B0}}{\rho_{\gamma 0}} \right]^2 \left( \frac{k}{k_m} \right)^{2(n_B+3)} e^{-\left(\frac{k}{k_m}\right)^2} \\ &\quad \times 6.30726 (n_B + 3.1)^{-0.992669}. \end{aligned} \quad (2.14)$$

The cross correlation two-point function of the magnetic energy density and anisotropic stress is determined by the dimensionless power spectrum given by

$$\mathcal{P}_{\langle\Delta_B\pi_B\rangle}(k, k_m) = \frac{3}{[\Gamma(\frac{n_B+3}{2})]^2} \left[\frac{\rho_{B0}}{\rho_{\gamma 0}}\right]^2 \left(\frac{k}{k_m}\right)^{2(n_B+3)} e^{-\left(\frac{k}{k_m}\right)^2} \int_0^\infty dz z^{n_B+2} e^{-2\left(\frac{k}{k_m}\right)^2 z^2} \int_{-1}^1 dx e^{2\left(\frac{k}{k_m}\right)^2 zx} (1-2zx+z^2)^{\frac{n_B-2}{2}} (-1+z^2+zx-(1+3z^2)x^2+3zx^3). \quad (2.15)$$

This is well fitted by the numerical fitting formula

$$\mathcal{P}_{\langle\Delta_B\pi_B\rangle}(k, k_m) = \frac{3}{[\Gamma(\frac{n_B+3}{2})]^2} \left[\frac{\rho_{B0}}{\rho_{\gamma 0}}\right]^2 \left(\frac{k}{k_m}\right)^{2(n_B+3)} e^{-\left(\frac{k}{k_m}\right)^2} \times (-3.43671) (n_B + 3.05)^{-0.329634n_B - 2.15842}. \quad (2.16)$$

The numerical fitting functions together with the full numerical solutions are shown in figure 1.

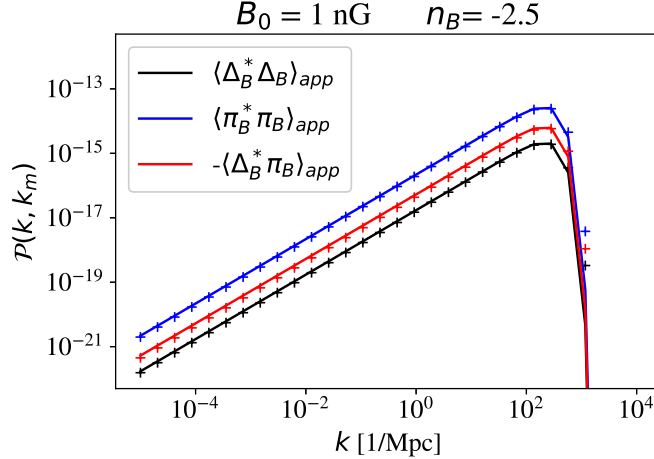


FIG. 1. Numerical fitting functions (solid lines)  $\langle X^*Y \rangle_{app}$ , with  $X, Y = \Delta_B, \pi_B$ , together with numerical evaluations (+) of the dimensionless power spectrum of the auto- and cross correlation functions,  $\mathcal{P}_{\langle\Delta_B\Delta_B\rangle}$ ,  $\mathcal{P}_{\langle\pi_B\pi_B\rangle}$  and  $-\mathcal{P}_{\langle\Delta_B\pi_B\rangle}$  for magnetic field parameters  $B_0 = 1$  nG,  $n_B = -2.5$ .

Initial conditions correspond to the compensated magnetic mode, an isocurvature type mode, or the passive magnetic mode, an adiabatic type mode (cf., e.g. [6]). The focus here is on the compensated magnetic mode [28].

### III. RESULTS

The numerical solutions for the CMB angular power spectra as well as the linear matter power spectrum have been obtained by modifying the publicly available Boltzmann solver code CLASS

[18]-[22]. The code has been modified in two ways. Firstly the non-thermal phase space distribution resulting from an added Gaussian peak as described in section II (cf. equation (2.1)) has been included. Secondly the contribution of the magnetic field has been added accordingly to the perturbation equations, the initial conditions for the compensated magnetic mode and the auto- and cross correlation functions for the magnetic energy density perturbation  $\Delta_B$  and the anisotropic stress  $\pi_B$  using a Gaussian window function as described in section II. For the latter ones the numerical approximations given in equations (2.12), (2.14) and (2.16) have been used. Numerical solutions are obtained for three different models:

- i.*) TH: a model with three thermal neutrinos each of the same mass which is chosen to be  $m_\nu = 0.167$  eV,
- ii.*) NT: a model with three non-thermal neutrinos with the same masses as in the thermal case (model *i.*) and the distribution function (2.1) setting the parameters to  $A = 0.1$ ,  $\sigma = 1.0$  and  $y_c = 9.489$ ,
- iii.*) TH+R-twin: the twin model of the three non-thermal neutrino model (*ii.*): three thermal neutrinos with extra relativistic degrees of freedom. In this model the neutrino masses are rescaled in order to ensure the same value of the neutrino density parameter  $\omega_\nu$  as in the non-thermal model (*ii.*).

The parameter values of the three non-thermal (NT) neutrino model (*ii.*) are chosen as way of example to study in particular the effect on the compensated magnetic mode. This results in the rather large, total number of relativistic degrees of freedom,  $N_{eff}^{NT} = 8.049$ . The three thermal neutrino model (*i.*) has the standard value,  $N_{eff}^{TH} = 3.04$ .

The cosmological background values are set to  $\omega_b = 0.022032$ ,  $\omega_c = 0.12038$ ,  $A_s = 2.215 \times 10^{-9}$  and  $\theta_s = 1.04136 \times 10^{-2}$ . which correspond to the Planck 13+WP bestfit values of the six-parameter base  $\Lambda$ CDM model [33]. Apart from  $\omega_c$  these cosmological background values are kept fixed in all numerical solutions. Additional relativistic degrees of freedom as obtained in the three non-thermal neutrino model (cf.  $N_{eff}^{NT}$  above for the particular choice of parameters for the distribution function equation (2.1)) postpone the beginning of the matter dominated epoch subsequently shortening the time remaining to photon decoupling. This results in larger amplitudes of the CMB anisotropies. Keeping the baryon density parameter unchanged, which is already constrained quite strongly by



LSS, .e.g., [2], for larger  $N_{eff}$  the epoch of radiation-matter equality  $z_{eq}$  can be adjusted to  $z_{eq}^{TH}$  of the three thermal neutrino model by changing  $\omega_c$  accordingly. This is indicated in the figures by the additional label  $z_{eq}^{TH}$ .

In figure 2 the angular power spectra of the CMB anisotropies are shown for the three thermal neutrino model (*i.*), the three non-thermal neutrino model (*ii.*) as well as the corresponding twin three thermal plus extra relativistic degrees of freedom (TH+R (twin)) model (*iii.*) for the adiabatic, primordial curvature mode and the compensated magnetic mode for  $B_0 = 3$  nG,  $n_B = -2.7$  as well as their ratios. As can be appreciated from figure 2 (*right*) the three non-thermal

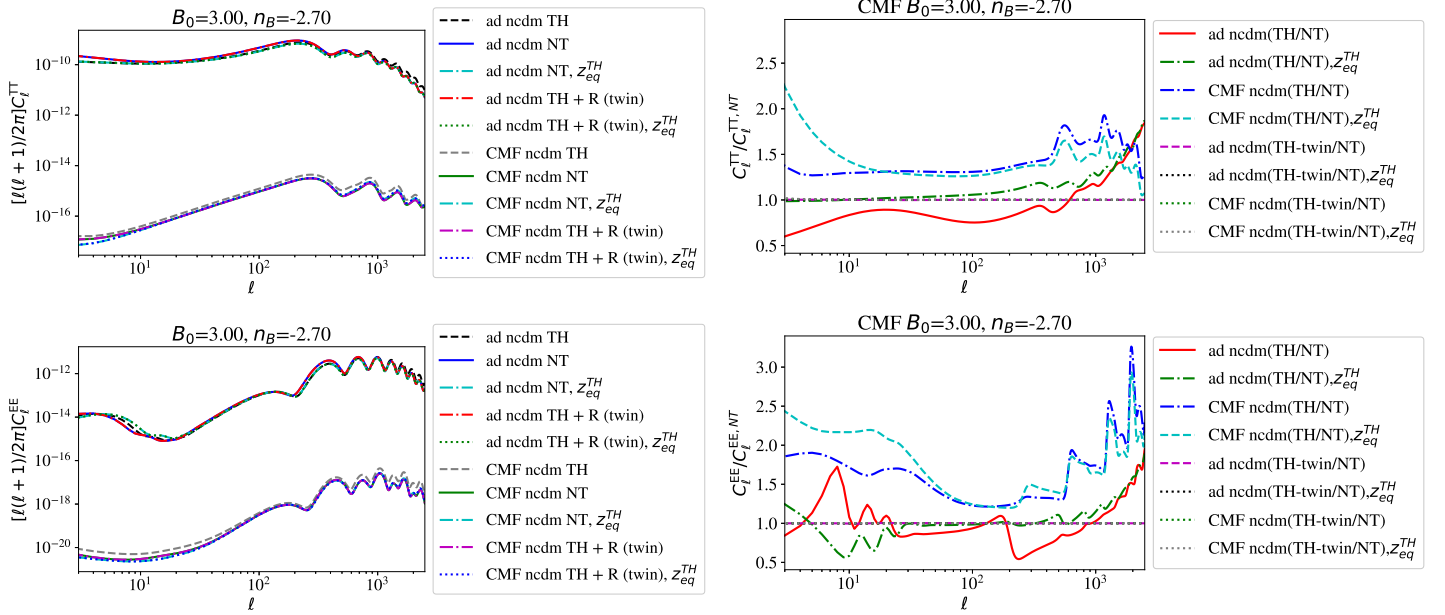


FIG. 2. T-mode (*upper panel*) and E-mode (*lower panel*) autorcorrelation angular power spectra (*left*) and ratios (*right*) of models with three thermal neutrinos (TH), three non-thermal neutrinos (NT), three non-thermal neutrinos (NT,  $z_{eq}^{TH}$ ) with  $\omega_c$  such that radiation-matter equality occurs at the same redshift as in the three thermal neutrino model  $z_{eq}^{TH}$  and their thermal twin models with extra relativistic degrees of freedom for the adiabatic mode (ad) and the compensated magnetic mode (CMF) with  $B_0 = 3$  nG,  $n_B = -2.70$ ).

neutrino model (*ii.*) is well described by the three thermal neutrinos plus extra relativistic degrees of freedom model (*iii.*). This holds for the adiabatic mode as well as the compensated magnetic mode.

To compare power spectra for the thermal and non-thermal cases it is useful to define the

corresponding relative change by

$$\frac{\Delta M}{M} \equiv \frac{M^{(NT, z_{eq}^{TH})} - M^{(TH)}}{M^{(TH)}} \quad (3.1)$$

where in the following  $M$  denotes the angular power spectra of the T-mode and of the E-mode auto correlation,  $C_\ell^{TT}$  and  $C_\ell^{EE}$ , respectively, as well as the linear matter power spectrum  $P(k)$ . In figure 3 the relative change of the CMB angular power spectra,  $\frac{\Delta C_\ell}{C_\ell}$  of the adiabatic as well as the compensated magnetic mode are shown for the T-mode and E-mode auto correlations for a set of different magnetic field parameters.

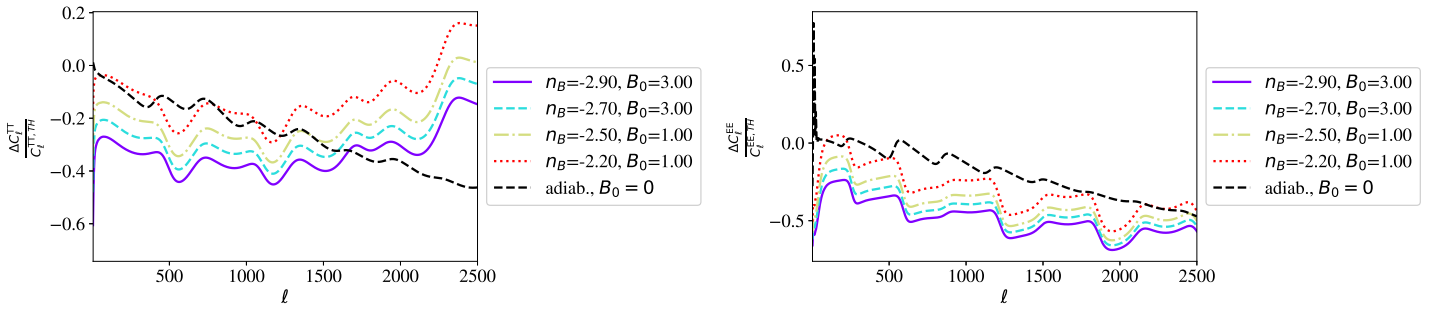


FIG. 3. Relative change of the CMB angular power spectra of the three non-thermal neutrinos (NT,  $z_{eq}^{TH}$ ) w.r.t. the three thermal neutrinos model (TH) (cf. equation (3.1)) for different choices of the magnetic field parameters for the compensated magnetic mode ( $B_0$ [nG],  $n_B$ ) as well as the adiabatic, primordial curvature mode.

In figure 4 the linear matter power spectra as well as the relative changes between the thermal and non-thermal neutrino models are shown for different values of the magnetic field parameters. In the presence of a magnetic field the magnetic Jeans length, corresponding to a wave number  $k_{mJ}$ , is a characteristic scale at which magnetic pressure support prevents gravitational collapse. However, as pointed out in [8] the density perturbation spectrum is cut-off at  $k_{mJ}$  only in a purely baryonic universe. As cold dark matter does not couple to the magnetic field the total matter power spectrum is flattened out but not cut-off at  $k_{mJ}$ . To model this correctly would require to include magnetohydrodynamical non linear effects which is beyond the scope of this paper.

As can be seen in figure 4 on small scales the effect of the Lorentz term is clearly visible. During the matter dominated era on subhorizon scales the linear matter power spectrum can be approximated by [36]

$$P_m^{(B)} = \frac{2\pi}{k^3} \left( \frac{k}{a_0 H_0} \right)^4 \frac{4}{225} (1 + z_{dec})^2 \left( \frac{\Omega_{\gamma,0}}{\Omega_{m,0}} \right)^2 \mathcal{P}_L(k) \quad (3.2)$$

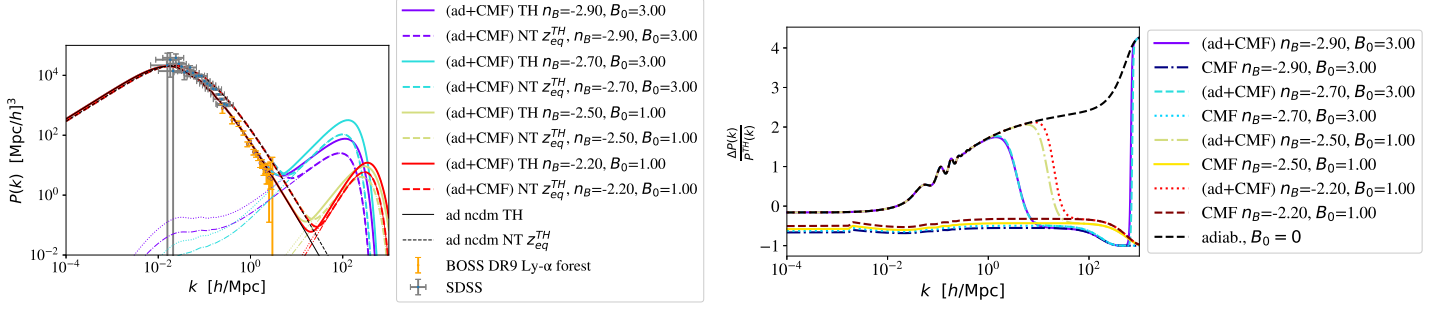


FIG. 4. Linear matter power spectrum for three thermal neutrinos (TH) and three non-thermal neutrinos (NT,  $z_{eq}^{TH}$ ) with distribution function (2.1) for different choices of the magnetic field parameters ( $B_0$ [nG],  $n_B$ ). *Left*: The total linear matter power spectrum of the adiabatic mode (ad) and the compensated magnetic mode (CMF) is shown together with data points from BOSS DR9 Ly- $\alpha$  forrest [34] and SDSS [35]. The light dotted and dashed-dotted lines indicate the three neutrino thermal magnetic mode and the three neutrino non-thermal pure magnetic mode solutions, respectively.  $z_{eq}^{TH}$  denotes that the cosmological parameters have been adjusted so that the redshift of radiation-matter equality in the non-thermal model is the same as that in the non-thermal one (see details in the text). *Right*: Relative change of the linear matter power spectrum w.r.t to the three thermal neutrino model (TH).

where  $\mathcal{P}_L(k)$  is the dimensionless power spectrum of the Lorentz term (cf. equation (2.5)). Keeping the redshift of radiation-matter equality fixed imposes (e.g., [2])

$$\Omega_{m,0} = \Omega_{\gamma,0} \left[ 1 + \frac{7}{8} \left( \frac{4}{11} \right)^{\frac{4}{3}} N_{eff}^{NT,TH-twin} \right] (1 + z_{eq}^{TH}), \quad (3.3)$$

where the equivalence of the three non-thermal neutrino model in terms of the three thermal neutrino plus extra relativistic degrees of freedom ((TH+R) (twin)) (cf. figure 2) is used. Since the three non-thermal neutrino model corresponds to additional relativistic degrees of freedom the effective coupling of the Lorentz term in the matter power spectrum is reduced. This can be observed in the numerical solutions in figure 4. In particular, the relative change w.r.t. the three thermal neutrino model in the linear matter power spectrum is negative as can be seen in figure 4 (*right*). In figure 4 (*left*) it can be appreciated that on larger scales the total linear matter power spectrum is dominated by the contribution of the adiabatic, primordial curvature mode. Thus its amplitude is enhanced in the three non-thermal neutrino model (*ii.*) On the contrary, on small scales the contribution of the compensated magnetic mode dominates over that of the adiabatic mode leading to a suppression of the total linear matter power spectrum in the three non-thermal neutrino model (*ii.*).

Moreover, there seem to be indications for a new degeneracy with the parameters of the magnetic field. For example, in figure 4 the numerical solutions for the magnetic field with  $B_0 = 3$  nG and for  $n_B = -2.9$  the three neutrino thermal model (*i.*) and for  $n_B = -2.7$  the three non-thermal neutrino model (*ii.*) are quite close. Thus in this case changing the magnetic field spectral index leads to a numerical solution of a three non-thermal neutrino model which effectively corresponds to that of a three thermal neutrino model.

In figure 4 (*left*) data points from BOSS DR9 Ly- $\alpha$  forest [34] and SDSS [35] have been included. The total linear matter power spectrum of the adiabatic, primordial curvature mode and the compensated magnetic mode for the numerical examples of the three neutrino non-thermal model just fit the error bars of the SDSS data points and are excluded by most of the BOSS data points. However, it should be kept in mind that the particular form of the non-thermal neutrino phase-space distribution function as well as the numerical values of the model parameters have been chosen to study the effects in general. A detailed parameter estimation study is left to future work.

#### IV. CONCLUSIONS

Models with three thermal light neutrinos and three non-thermal light neutrinos with the same degenerate mass configuration have been studied in the presence of a primordial stochastic magnetic field. The non-thermal neutrino distribution function is modelled by a Fermi-Dirac distribution with an additional Gaussian peak. This type of distribution could be the result of a scalar particle decaying into neutrinos after decoupling of the neutrinos of the standard model of cosmology [13]. The numerical solutions for the angular power spectra of the CMB anisotropies as well as the linear matter power spectrum have been found by modifying the CLASS code accordingly. There is a known degeneracy between (light) neutrino masses  $m_0$ , the cold dark matter density parameter  $\omega_c$  and the number of relativistic degrees of freedom  $N_{eff}$  for  $\Lambda$ CDM models leading to an equivalent, effective description of models including non-thermal neutrinos in terms of a twin thermal neutrino model with extra relativistic degrees of freedom [13]. Here it has been found that this effective description can be extended to models with non-thermal neutrinos in the presence of a stochastic magnetic field. Moreover, an additional degeneracy with the magnetic field parameters has been observed in the numerical solutions allowing to connect for the same magnetic field amplitude a three thermal neutrino model with a three non-thermal neutrino model by changing the magnetic

field spectral index.

Moreover, it is found that the amplitude of the linear matter power spectrum of the three neutrino non-thermal pure compensated magnetic mode is suppressed in comparison to the one in the three neutrino thermal pure compensated magnetic mode model. This is the opposite behaviour of the adiabatic, primordial curvature mode where the amplitude is larger in the case of the three non-thermal neutrino model. The suppression of the matter perturbation of the three non-thermal neutrino compensated magnetic mode is related to the diminished coupling to the Lorentz term because of a larger cold dark matter density parameter. Thus magnetic field spectra with larger amplitudes or stronger tilt can be compensated by light neutrinos with a non-thermal phase space distribution.

## V. ACKNOWLEDGMENTS

Financial support by Spanish Science Ministry grant PGC2018-094626-B-C22 (MCIU/AEI/FEDER, EU) and Basque Government grant IT979-16 is gratefully acknowledged.

- 
- [1] P. A. Zyla et al. (Particle Data Group), *PTEP* **2020**, 083C01 (2020).
  - [2] J. Lesgourgues, G. Mangano, G. Miele, and S. Pastor, *Neutrino Cosmology* (Cambridge University Press, 2013), ISBN 978-1-108-70501-1, 978-1-139-60341-6.
  - [3] S. Hannestad, *Prog. Part. Nucl. Phys.* **65**, 185 (2010), 1007.0658.
  - [4] C. Giunti and C. W. Kim, *Fundamentals of Neutrino Physics and Astrophysics* (Oxford University Press, 2007), ISBN 978-0-19-850871-7.
  - [5] A. D. Dolgov, *Phys. Rept.* **370**, 333 (2002), hep-ph/0202122.
  - [6] J. R. Shaw and A. Lewis, *Phys. Rev.* **D81**, 043517 (2010), 0911.2714.
  - [7] S. K. Sethi and K. Subramanian, *Mon. Not. Roy. Astron. Soc.* **356**, 778 (2005), astro-ph/0405413.
  - [8] E.-j. Kim, A. Olinto, and R. Rosner, *Astrophys. J.* **468**, 28 (1996), astro-ph/9412070.
  - [9] I. Wasserman, *Astrophys. J.* **224**, 337 (1978).
  - [10] P. A. R. Ade et al. (Planck), *Astron. Astrophys.* **594**, A19 (2016), 1502.01594.
  - [11] J. Chluba, D. Paoletti, F. Finelli, and J.-A. Rubiño-Martín, *Mon. Not. Roy. Astron. Soc.* **451**, 2244 (2015), 1503.04827.
  - [12] K. E. Kunze and E. Komatsu, *JCAP* **1506**, 027 (2015), 1501.00142.

- [13] A. Cuoco, J. Lesgourgues, G. Mangano, and S. Pastor, Phys. Rev. D **71**, 123501 (2005), astro-ph/0502465.
- [14] E. Bertschinger (1995), astro-ph/9506070.
- [15] U. Seljak and M. Zaldarriaga, Astrophys. J. **469**, 437 (1996), astro-ph/9603033.
- [16] A. Lewis, A. Challinor, and A. Lasenby, Astrophys. J. **538**, 473 (2000), astro-ph/9911177.
- [17] M. Doran, JCAP **10**, 011 (2005), astro-ph/0302138.
- [18] J. Lesgourgues (2011), 1104.2932.
- [19] D. Blas, J. Lesgourgues, and T. Tram, JCAP **1107**, 034 (2011), 1104.2933.
- [20] J. Lesgourgues (2011), 1104.2934.
- [21] J. Lesgourgues and T. Tram, JCAP **1109**, 032 (2011), 1104.2935.
- [22] J. Lesgourgues and T. Tram, JCAP **1409**, 032 (2014), 1312.2697.
- [23] P. Crotty, J. Lesgourgues, and S. Pastor, Phys. Rev. D **67**, 123005 (2003), astro-ph/0302337.
- [24] S. Bashinsky and U. Seljak, Phys. Rev. D **69**, 083002 (2004), astro-ph/0310198.
- [25] Z. Hou, R. Keisler, L. Knox, M. Millea, and C. Reichardt, Phys. Rev. D **87**, 083008 (2013), 1104.2333.
- [26] B. Follin, L. Knox, M. Millea, and Z. Pan, Phys. Rev. Lett. **115**, 091301 (2015), 1503.07863.
- [27] T. Kahniashvili and B. Ratra, Phys. Rev. **D71**, 103006 (2005), astro-ph/0503709.
- [28] K. E. Kunze, Phys. Rev. **D83**, 023006 (2011), 1007.3163.
- [29] D. Paoletti, F. Finelli, and F. Paci, Mon. Not. Roy. Astron. Soc. **396**, 523 (2009), 0811.0230.
- [30] K. Jedamzik, V. Katalinic, and A. V. Olinto, Phys. Rev. **D57**, 3264 (1998), astro-ph/9606080.
- [31] K. Subramanian and J. D. Barrow, Phys. Rev. **D58**, 083502 (1998), astro-ph/9712083.
- [32] K. E. Kunze, Phys.Rev. **D85**, 083004 (2012), 1112.4797.
- [33] P. A. R. Ade et al. (Planck), Astron. Astrophys. **571**, A16 (2014), 1303.5076.
- [34] S. Chabanier, M. Millea, and N. Palanque-Delabrouille, Mon. Not. Roy. Astron. Soc. **489**, 2247 (2019), 1905.08103.
- [35] M. Tegmark and M. Zaldarriaga, Phys. Rev. D **66**, 103508 (2002), astro-ph/0207047.
- [36] K. E. Kunze, Phys. Rev. D **89**, 103016 (2014), 1312.5630.